Tuning the potential drop at graphene/protic ionic liquid interface by molecular structure engineering

Electrochimica Acta 458 (2023) 142344

Contents lists available at ScienceDirect

Electrochimica Acta

journal homepage: www.journals.elsevier.com/electrochimica-acta

Tuning the potential drop at graphene/protic ionic liquid interface by molecular structure engineering

Federico Raffone [a,b,*], Andrea Lamberti [a,b], Giancarlo Cicero [a,*]

[a] Department of Applied Science and Technology, Politecnico di Torino – Corso Duca degli Abruzzi, 24, 10129 Turin, Italy
[b] Center for Sustainable Future Technologies CSFT@Polito, Istituto Italiano di Tecnologia - Via Livorno, 60, 10144 Turin, Italy

ARTICLE INFO

Keywords:
Molecular dynamics
Ionic liquids
Electrical double layer
Solid/liquid interface

ABSTRACT

Ionic liquids (ILs) have been extensively employed in many applications involving interfaces with carbon-based electrodes, such as energy storage devices (batteries or supercapacitors) or electrocatalytic devices, where the way each ion of the IL interacts with the electrode has a strong impact on the overall performance of the device. For instance, the amount of potential difference between the electrode and the bulk of the IL is highly sensitive to the IL composition and it is directly related to the device capacitance. The selection of the most suited pair of ions often proceeds by time-consuming and costly trial-and-error approaches. It is necessary to understand the atomistic features of the interface to determine the effect of each ion on the potential drop. By classical molecular dynamics simulations, we show that it is possible to quickly infer the interface potential arising at the carbon electrode by carefully inspecting the molecular structure of the IL. The ion orientation at the interface is, in fact, determined by the distribution of charges within the molecules. Depending on where charges are located, ions can either lie flat or perpendicular to the interface to minimize the surface energy. The interface potential is found to be mainly determined by ion–ion interactions dictating the interface energy minimization process, whereas ion–electrode interactions are found to enforce higher ordering and charge layers stacking but not to induce selective adsorption of an ion over the other.

1. Introduction

Ionic liquids (ILs) are salts naturally melt at temperatures smaller than 100 °C [1]. This feature sets ILs apart from conventional materials. Generally, ILs show high ionic density, a low vapor pressure and a wide electrochemical stability window [2], that make them highly desirable in a number of applications. Moreover, the IL properties (viscosity, thermal and chemical stability, etc.) and the way ILs interact with external materials (electrodes or gases) can be highly tuned by changing the constituent ions [3,4]. With the proper selection of ions, it is possible to employ ILs as electrolyte for batteries [5,6], capacitors and supercapacitors [7–11], catalyst, electrolyte or ionic conductive membrane for fuel cells [12–14], absorbent agent for gas capture [15–17] or solvent for biological media [18]. However, the search for the most suited pair of ions for a given application is still a trial-and-error process. It would be highly beneficial, in order to speed up the optimization of device performances, to identify specific rules which can guide the researchers in the selection of the right combination of ions. For instance, in gas capture IL must be designed so that the ion arrangement at the interface facilitates the motion of the molecules from the gas to the IL bulk [19]. On the other hand, for batteries and supercapacitors a high capacitance, i.e. a small potential drop at the electrode/IL interface, is very desirable. In this respect, it would be fundamental to understand what features of the ionic liquid determine the potential drop at the interface with the electrodes. In particular, IL are often interfaced with carbon based electrodes such as activated carbon [20], carbon nanotubes [21], and graphene [22] because they are easily processable, electrochemically inert and low cost [23]. For these technological aspects, the comprehension of the factors affecting the carbon electrode/IL interface holds extreme relevance.

A large amount of theoretical work has been done to predict how molecules arrange at the electrode interface (in the double layer) and how the potential and capacitance are affected. Mean field theories revealed the existence of two regimes, overscreening and crowding, characterized by distinct ionic arrangements at the interface [3,24,25]. In the former, which is typical of low bias, the ions are distributed in alternating layers of positive and negative charge causing oscillations in the electric potential. The charge of the first layer is higher in absolute

* Corresponding authors.
E-mail addresses: federico.raffone@polito.it (F. Raffone), giancarlo.cicero@polito.it (G. Cicero).

https://doi.org/10.1016/j.electacta.2023.142344
Received 30 December 2022; Received in revised form 14 March 2023; Accepted 31 March 2023
Available online 24 April 2023

value to the charge stored in the electrodes. The second layer opposes to such a charge with a smaller amount of the opposite polarity. Charge oscillations continue slowly decaying until bulk neutrality is reached. The latter case takes place at high bias and is characterized by an accumulation of counterions in the closest few layers at the interface [25]. Despite of their great success, mean field models cannot capture aspects like the complex structure of large ions and the weak interactions with the electrode such as carbon–carbon π-stacking or other van der Waals (vdW) interactions. Ions are, in fact, often characterized by complex molecular structures and each part of the molecule interacts differently with the environment. In particular, the presence of an electrode, even when uncharged, can significantly influence the way ions arrange away from the electrode because vdW interactions lead to an alteration of the electric double layer. Classical molecular dynamics (MD) simulations are able to include the effects that are missing in mean field theory calculations [26–29]. One of the aspects highlighted by MD is ion selective adsorption on carbon electrode/IL interfaces [26,30]. Usually, one of the two IL ions is found to stick on the surface, thus providing a significant potential drop at the point of zero charge. The effect is attributed to the weak interactions between graphitic electrode and carbon rich parts of the adsorbed ion. Nevertheless, MD, so far, has mainly provided indications on a case-by-case basis: each combination of ions in the IL leads to a specific ion distribution/potential drop. A general guidance for the selection of the right IL components for the application is still missing.

In this work we demonstrate that it is possible to predict the potential drop and the molecular arrangement at the carbon electrode/IL interface by careful inspection of the structure of the IL ions and by identifying the presence of polar and/or non-polar centers in their structure. Such centers directly influence the way molecules orient at the vacuum/IL interface that is found to be akin to the one observed at the carbon electrode/IL interface. Moreover, we show how selective adsorption on carbon surfaces is not inherently a consequence of vdW interactions with the electrode but rather a consequence of the existence of a surface in the IL that forces polar parts of the ions to point toward the bulk while non-polar parts are repelled away toward the IL surface. Van der Waals interactions do not determine the type of ionic species directly in contact with the electrode surface but they mainly affect their amount.

2. Methods

Classical molecular dynamics simulations were carried out with LAMMPS [31]. The ionic liquid ions used in this work ([DBUH$^+$], [Im$^-$], [$CH_3NH_3^+$] and [NO_3^-]) were described by means of the GAFF2 potential [32], already proved to accurately predict ILs properties [33]. Electrostatic point charges on the atoms of the ions were calculated with the aid of Hartree-Fock simulations with a 6-31G(d) basis set using GAMESS software [34]. The Hartree-Fock calculations provided the electrostatic potential of the ion that is then converted in the most suited point charges thanks to the RASP algorithm [35]. Ion charges resulting from Hartree-Fock calculations were scaled by 0.8 as typically done to avoid artificial overstructuring of the IL [33,36]. The force field used to describe the electrode carbon is a 12-6 Lennard-Jones with paraments taken from GAFF2.

In the case of the carbon electrode/IL interface, the simulation box contained two parallel graphene planes acting as electrodes. Carbon atoms were frozen in a two dimensional sheet arrangement, but the position of the graphitic plane was allowed to vary. The graphene sheets covered an area of 30 Å x 30 Å. 300 pairs of [DBUH$^+$][Im$^-$] or 450 pairs of [$CH_3NH_3^+$][NO_3^-] were placed between the two electrodes. To find the equilibrium distance between the graphene electrodes containing the IL, ambient pressure was applied to one of the two graphene layers pushing against the other [37,38]. The system was first equilibrated at 600 K for 10 ns. High temperature is commonly used to accelerate phenomena like mixing [39–42]. Temperature was then lowered to 400 K and 5 ns were given to the system to readjust before monitoring the position of the pressured graphene for additional 5 ns. The graphene electrodes were then fixed at the average distance obtained from the previous run and the system was further equilibrated for 2 ns. A production run of 40 ns followed to collect statistics and calculate the equilibrium quantities. For the study of the vacuum/IL interface, the final configuration of the electrode/IL system was taken and the graphene electrodes removed. The system was allowed to equilibrate for 5 ns and then data was extracted for 40 ns. The temperature was maintained with a Nosé-Hoover thermostat and the system was integrated with a timestep of 1 fs. Periodic boundary conditions were applied in all directions. To prevent replica interactions a vacuum layer of, at least, 100 Å was placed in the direction perpendicular to the electrodes.

The charge distribution as function of the distance from the electrode was calculated sampling the trajectory every 0.05 ns and assigning to each atom a Gaussian function with height proportional to the atom charge. The related electric potential was calculated applying Poisson's equation with periodic boundary conditions.

For the calculation of the angular orientation on the ions with respect to the surface, the same 0.05 ns sampled trajectory was used. The orientation was obtained by calculating the cosine of the angle between the vector perpendicular to the electrode surface and the vector assigned to each ion as indicated in Fig. 1. The mass center coordinates of the molecule were taken to calculate the distance from the surface. For all postprocessing, the data from the two IL/electrode interfaces were averaged to increase statistics, because they are equivalent by symmetry.

The binding energy (BE) between ions and graphene electrode was calculated as difference between the relaxed interacting graphene/single ion system and the non-interacting one where the electrode and the ion were placed 100 Å apart from each other.

3. Results and discussion

3.1. Understanding the effect of IL-carbon electrode interactions

We begin our analysis by investigating the graphene/IL interface using a protic IL, [DBUH$^+$][Im$^-$] (1,8-Diazabicyclo[5.4.0]undec-7-ene imidazole), known for applications in room temperature CO_2 and H_2S capture [16,17]. Fig. 1 shows the structure of the [DBUH$^+$][Im$^-$] ions. The IL is interfaced with graphene, a prototypical material for carbon-based electrodes [43].

From Fig. 2a (blue line) it is possible to notice that, even for uncharged contacts, there is a significant potential difference between the electrode and the bulk of the IL. Such potential, arising when there is no surface charge on the electrode, is referred as potential of zero charge. The large difference is mainly given by the formation of a strong dipole at the interface formed by a first positive charge layer and a negative second layer (see Fig. 2b, blue line). Positively and negatively charged layer alternation continues beyond the first dipole, decaying as the distance from the electrode increases and giving rise to the well-known oscillations that characterize overscreening. By inspecting the ion orientation at the surface (Fig. 2c), the origin of the charge distribution can be understood. [DBUH$^+$] tends to mainly be adsorbed flat on the surface (violet areas between 4 and 4.5 Å for cosθ around 0 in Fig. 2c) forming the first positive charge peak. [DBUH$^+$] is also found pointing its positive nitrogen atom toward the IL bulk farther away from the interface. On the contrary, [Im$^-$] is oriented in such a way that its negatively charged center points away from the surface and toward the liquid phase while leaving the non-polar carbon atoms in proximity of the surface (see area at cosθ equal 1 around 4.5 Å in Fig. 2c). Given the high content of carbon in [DBUH$^+$], its selective absorption on the graphene surface could be caused by strong π-stacking and other vdW interactions. [DBUH$^+$] binding energy is, indeed, found to be −0.69 eV, whereas [Im$^-$] binding energy when flat is only −0.37 eV. To check the validity of this interpretation, we performed a hypothetical in-silica experiment: we reduced the value of the parameters determining the

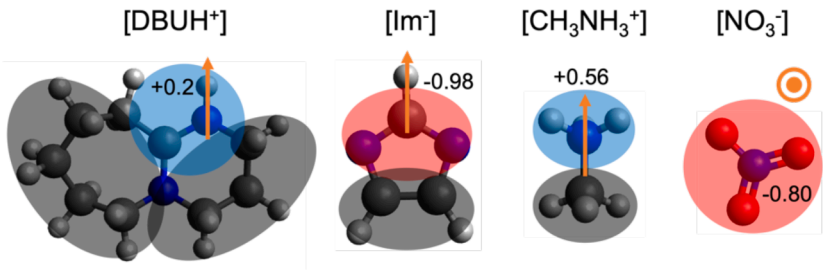

Fig. 1. Ball and stick representation of the IL molecules used in the study. Carbon, hydrogen, oxygen and nitrogen atoms are respectively shown in black, white, red and blue. The black shaded areas are indicative of the non-polar regions of the molecules, whereas blue and red areas indicate respectively positive and negative charged centers. The nearby number represents the amount of charge of each area in electron charge units (each ion carries a total charge of 0.8 |e|). The orange arrows indicate the vectors used in the orientation analysis of Fig. 2c, Fig. 3c and Fig. 4c.

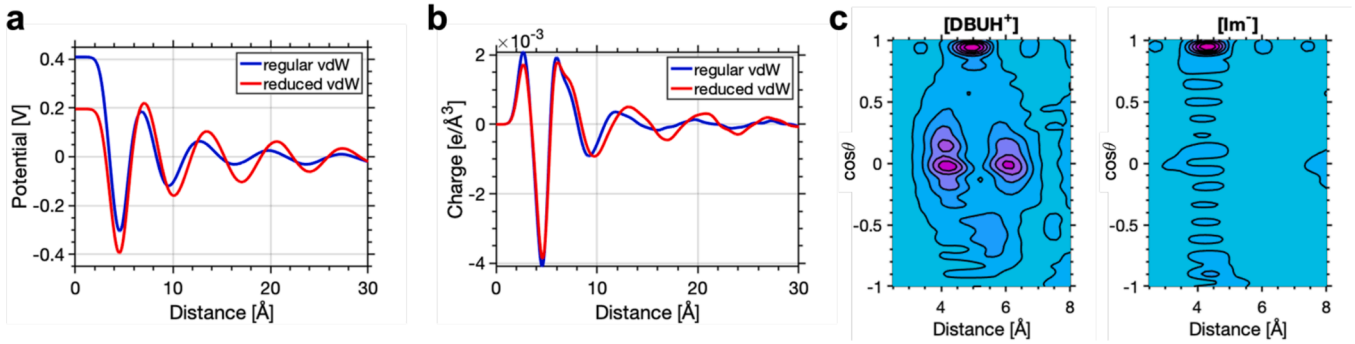

Fig. 2. Potential (a) and charge distribution (b) as function of the distance from the graphene electrode. The blue lines indicate the simulation where the vdW interactions between [DBUH$^+$] and graphene are unaltered. The red lines indicate the case where the vdW interactions are intentionally reduced. [DBUH$^+$] and [Im$^-$] orientation at the interface with graphene with unaltered vdW interactions (c). The orientation is calculated as cosine of the angle formed by the interface normal vector and the vectors associated to a given molecule as reported in Fig. 1. The magenta color indicates a higher percentage of ions sharing the same angular orientation, whereas cyan a less probable angle.

strength of the vdW interactions between [DBUH$^+$] and graphene to the point where both ions shared the same binding energy. Results are shown in Fig. 2a and b (red lines). The reduction of the binding energy of [DBUH$^+$] has only a quantitative effect on the potential difference between electrode and IL bulk but has no qualitative effect. There is a lesser amount of [DBUH$^+$] lying on the electrode surface but the overall orientation of the ions is the same and, as consequence, there is a smaller potential variation (compare Fig. 2c to Fig. S1 in Supporting Information). We conclude that the potential of zero charge is not qualitatively affected by selective adsorption, which is a result of interplay between ions and substrate interactions. If the type of species at the surface are not determined by ion–electrode interactions, then they must be affected by ion–ion interactions.

3.2. *Determining the origin of ion arrangement at the electrode/IL interface*

To investigate solely the effects of the ion–ion interaction without any influence from the electrode, a vacuum/[DBUH$^+$][Im$^-$] interface was studied and compared with the previous graphene/[DBUH$^+$][Im$^-$] interface. Results shown in Fig. 3a highlight that the typical oscillations in the potential due to overscreening [44] are significantly reduced. The reason is that the presence of a wall automatically induces a more ordered structure as atoms gravitate around the minimum of the Lennard-Jones potential of the electrode atoms. When the boundary is looser like in the case of vacuum, highly defined charged layers cannot form. Nevertheless, the main features characterizing the interface with graphene are still present. The bulk potential is still significantly lower than that at the interface as there is still an accumulation of positive charges at the boundary as seen in Fig. 3b. The first and second charge peaks are much broader compared to the graphene/IL interface but they resemble the same trend. The analogy between the two interfaces is visible also comparing the ion orientation at the interface (Fig. 2c and Fig. 3c).

Similarly to the graphene interface, in the case of vacuum [DBUH$^+$] is found to mainly lie flat at the IL surface. The distribution is less

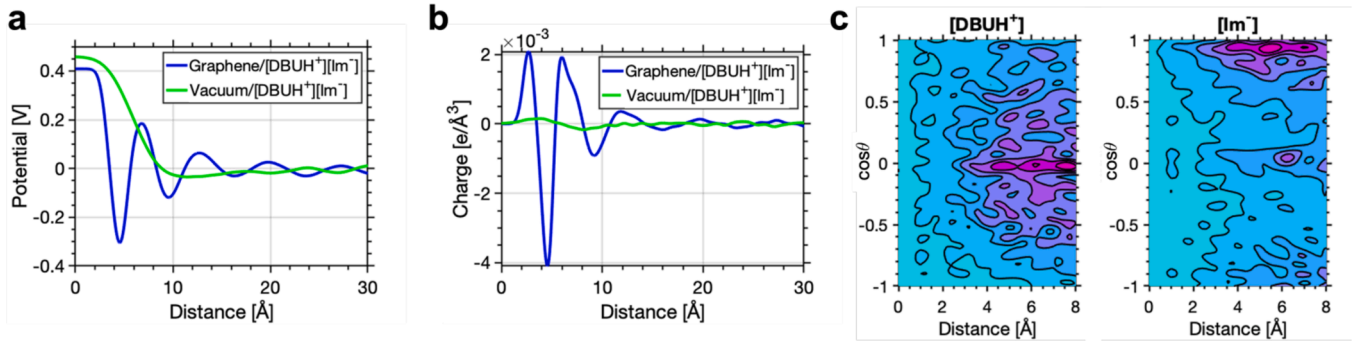

Fig. 3. Potential (a) and charge distribution (b) as function of the distance from the interface for graphene/[DBUH$^+$][Im$^-$] (blue), for reference, and vacuum/[DBUH$^+$][Im$^-$] (green). [DBUH$^+$] and [Im$^-$] orientation for the vacuum/[DBUH$^+$][Im$^-$] interface (c).

pronounced due to the looser ordering of the molecules but the orientation is preserved. The portion of [DBUH$^+$] from the inner layer pointing toward the liquid phase in the graphene/IL interface is missing, possibly because of the broader distribution of the counterion to which [DBUH$^+$] is connected by coulomb attraction. At the interface with vacuum, [Im$^-$] is still found to direct its nitrogen atoms towards the liquid bulk phase similarly to the interface with graphene. Also in this case,there is a less sharp distribution but the similarity in the general trend is evident.

We deduce that the peculiar ordering of the molecules at the interface is a consequence of the existence of a surface or an interface (making the liquid no longer isotropic). When an interface is formed, the internal energy has to be minimized by rearrangement of the molecular orientation. Coulombic ion–ion interactions are the strongest and dictate the minimization process. As such, the highly charged centers of the ions are more prone to be directed toward the liquid bulk phase where the counterions are. The non-polar ends of molecules, instead, tend to be pushed away from the inner liquid layer as they create space between opposite polarity ions weakening the cation–anion coulombic attraction. Consistently, experimental studies on the interface between vacuum and IL reported an accumulation of carbon containing groups at the interface [45,46]. Additionally, the interfaces that water forms, were reported to show a similar behavior to the ones of ILs. The water/-hydrophobic substrate interface was found to preserve the features of the water/vapor interface due to the strong hydrogen bonding among molecules [47]. Because the origin of the ordering in ILs is the ion–ion interaction, orientations like the ones found for graphene are expected also for other materials, if there are no local polarized areas, such as highly charged functional groups. Other materials will possibly lead to a different amount of ions, proportional to the ion–electrode van der Waals interactions, while preserving the same ordering.

In our case, [Im$^-$] possesses an asymmetric charge distribution due to the presence a strong charge center around the nitrogen atoms accumulating up to -0.98 |e| (see Fig. 1) that is opposed to a non-polar side constituted by carbon atoms. Energy minimization at the interface imposes the charged side to stay closer to the bulk. [DBUH$^+$] is, instead, characterized by a weak charge center ($+0.2$ |e|) which is surrounded by non-polar atoms (Fig. 1). Such characteristic makes more likely for the cation to lie flat at the interface and form the first positive charge liquid layer. The fact that the charged center is so weak implies that the remaining positive charge of the ion (roughly $+0.6$ |e| in our simulations) is spread throughout the molecule, especially on the hydrogen atoms. Still the cation is also found to point its charged center toward the liquid bulk partially overlapping with [Im$^-$] but its large size prevents it to have a strong impact on the charge distribution of the first dipole.

The similar behavior of vacuum and graphene interfaces arises from the fact that carbon atoms both characterize the non-polar areas of the ions (detrimental for close coulombic attraction among ions) and show affinity with the electrode. Additionally, graphene surfaces do not show charged functional groups that could locally disrupt the ordering through specific Coulomb interactions or by locally polarizing the interface ions. It is then possible to predict the general features of potential of zero charge of the graphene/IL interface simply by looking at the behavior at the vacuum/IL interface. The ion distribution at interface can be predicted by the way polar/non-polar areas are distributed in the ions composing the IL. Moreover, the ion distribution at $V = 0$ is likely to affect the behavior of the interface also when polarized. It was shown that the accumulation of positive ions at the interface can persist also when the electrode is positively biased [30]. The presence of one ionic species can have significant impact on the device performance. For instance, Rudnev et al. have proven that specific cation adsorption plays a crucial role in catalyzing CO_2 electroreduction [48]. So, indications provided in this work at the potential of zero charge can potentially be applied to electrified interfaces, as well.

3.3. Tweaking the potential at the interface

To further strengthen our point, we tested a different ionic liquid, monomethylammonium nitrade ([$CH_3NH_3^+$][NO_3^-]) [45], whose ions show very different properties with respect to [DBUH$^+$][Im$^-$]. In particular, the cation [$CH_3NH_3^+$], as shown in Fig. 1, has a strongly asymmetric charge distribution characterized by a positively charged end ($+0.56$ |e|) opposed to a non-polar end, just like previously was observed for the [Im$^-$] anion. [NO_3^-], instead, has its negative charge distributed throughout the whole molecule. Based on these features we expect the two ions to orient in the opposite way with respect to what observed for [DBUH$^+$][Im$^-$]. Fig. 4c confirms our hypothesis showing that, in [$CH_3NH_3^+$][NO_3^-], it is now the cation that lies perpendicular to the surface (purple areas for cosθ equal 1), given its high directionality, whereas the anion, due to the spread charge, rather stay flat (areas around ±1). Comparing the orientation of [DBUH$^+$][Im$^-$] in Fig. 2c to those of [$CH_3NH_3^+$][NO_3^-] in Fig. 4c it is evident the role of charge distribution and ion–ion interaction in dictating the molecules orientation at the interface. The influence on the potential profile can be seen in Fig. 4a where the potential at the interface is significantly lower than that of [DBUH$^+$][Im$^-$]. Therefore, we showed how, by changing the characteristics of the ions in terms of structure and molecular charge distribution, it is possible to engineer the interface potential to the application needs. We notice, however, that the potential profile at the electrode, in this case, is not exactly specular compared to [DBUH$^+$][Im$^-$]. The reason of such behavior lies in the position at the interface of the hydrogen atoms that must be accounted for when predicting the potential at the interface. Hydrogen atoms in [$CH_3NH_3^+$], due to their reduced dimension, can move closer than the oxygen atoms from [NO_3^-] to the electrode surface (see Fig. 4d for a plot of the atom distribution as function of the distance from the surface). Even if hydrogen atoms are only slightly positive, the first charge layer is found to be positive as shown is Fig. 4b. The more pronounced negative peak originated from [NO_3^-] sits immediately after. Consequently, there is an initial potential oscillation that opposes to the one given by the dipole formed by the flat [NO_3^-] and the perpendicular [$CH_3NH_3^+$] reducing the magnitude of the expected drop.

4. Conclusions

In conclusion, although the mechanisms that dictate the interfacial distribution and orientation of molecules and the consequent induced potential variation are complex, some molecular features are important in determining the electrical feature of the IL/graphene interface. Given the strong ion–ion interactions in ILs, charge centers in molecules play a major role in the positioning of ions at the interface. We found that the location of the ion charge centers determines whether the molecule will preferentially orient perpendicularly or parallelly to the interface. For instance, an amphiphilic molecule, characterized by a polar/non-polar axis, is more prone to assume this orientation. This tendency is also enhanced by the fact that non-polar areas of the molecules tend to be repelled away from the IL bulk as they hinder cation–anion Coulomb attraction by creating space among the molecules. On the contrary, molecules having evenly spread charge tend to show the opposite behavior. There is no preferential direction for the molecule to interact with the nearby ions, so they are left at the edges of the IL typically lying flat on the surface. Ion–electrode interactions, such as π-stacking or other vdW forces, were found instead to increase the amount of molecule that show high affinity with the electrode carbon atoms but not to change the orientation of the species at the surface, contrary to the hypothesis that population at the interface is driven by selective adsorption of one of the two ions. The role of carbon electrodes has been identified in primarily enhancing the ion ordering at the interface. This creates stacked layers of opposite polarity giving rise to the well-known oscillating potential next to the surface. Because of the secondary role of the electrode, when studying the interface, the focus is then shifted from

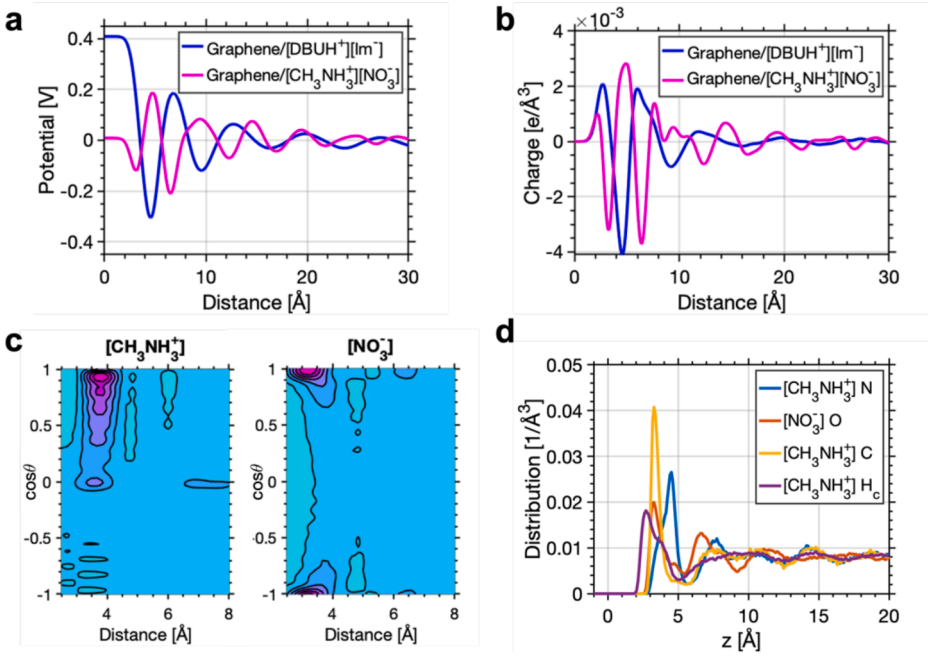

Fig. 4. Potential (a) and charge distribution (b) as function of the distance from the interface for graphene/[DBUH$^+$] [Im$^-$] (blue), as reference, and graphene/[$CH_3NH_3^+$][NO_3^-] (magenta). [$CH_3NH_3^+$] and [NO_3^-] orientation for the graphene/ [$CH_3NH_3^+$] [NO_3^-] interface (c). Distribution of selected atom species (nitrogen in [$CH_3NH_3^+$], oxygen in [NO_3^-], carbon and the connected hydrogens in [$CH_3NH_3^+$]) as function of the distance from the electrode (d). Distributions are normalized to the number of atoms of the same species in an ion.

the understanding of the specific ion–electrode interaction toward the understanding how IL itself behaves at the surface. The indications we provided on the molecule orientation give a way to infer the possible interface potential. Predictions on the interface potential were gathered by studying protic ionic liquids, [DBUH$^+$][Im$^-$] and [$CH_3NH_3^+$][NO_3^-], but they can be potentially applied to aprotic ILs, as well, because the potential is mainly affected by the charge distribution in the molecules composing the IL. Such information can be rapidly obtained by careful chemical analysis of the molecule structure or by a simple *ab initio* simulation of the single molecules, avoiding time-consuming and expensive trial-and-error approaches. The identification and selection of the correct couple of ions for the realization of supercapacitors, fuel cells, or gas capture devices is then a much easier and quicker process that can lead to major speed up of the research in these applications.

CRediT authorship contribution statement

Federico Raffone: Conceptualization, Methodology, Writing – review & editing. **Andrea Lamberti:** Conceptualization, Writing – review & editing. **Giancarlo Cicero:** Conceptualization, Methodology, Writing – review & editing.

Declaration of Competing Interest

The authors declare that they have no known competing financial interests or personal relationships that could have appeared to influence the work reported in this paper.

Data availability

Data will be made available on request.

Acknowledgments

This result is part of a project that has received funding from the European Research Council (ERC) under the European Union's ERC Starting Grant. Grant agreement "CO2CAP" No. 949916. We acknowledge the CINECA award under the ISCRA initiative and HPC@POLITO for the availability of high-performance computing resources and support.

Supplementary materials

Supplementary material associated with this article can be found, in the online version, at doi:10.1016/j.electacta.2023.142344.

References

[1] T.L. Greaves, C.J. Drummond, Protic ionic liquids: evolving structure-property relationships and expanding applications, Chem. Rev. 115 (20) (2015) 11379–11448, https://doi.org/10.1021/acs.chemrev.5b00158.
[2] R.L. Vekariya, A review of ionic liquids: applications towards catalytic organic transformations, J. Mol. Liq. 227 (2017) 44, https://doi.org/10.1016/j.molliq.2016.11.123.
[3] M.V. Fedorov, A.A. Kornyshev, Ionic liquids at electrified interfaces, Chem. Rev. 114 (5) (2014) 2978–3036, https://doi.org/10.1021/cr400374x.
[4] Z. Lei, B. Chen, Y.M. Koo, D.R. Macfarlane, Introduction: ionic Liquids, Chem. Rev. 117 (10) (2017) 6633–6635, https://doi.org/10.1021/acs.chemrev.7b00246.
[5] N. Böckenfeld, M. Willeke, J. Pires, M. Anouti, A. Balducci, On the use of lithium iron phosphate in combination with protic ionic liquid-based electrolytes, J. Electrochem. Soc. 160 (4) (2013) A559–A563, https://doi.org/10.1149/2.027304jes.
[6] S. Menne, J. Pires, M. Anouti, A. Balducci, Protic ionic liquids as electrolytes for lithium-ion batteries, Electrochem. Commun. 31 (2013) 39–41, https://doi.org/10.1016/j.elecom.2013.02.026.
[7] L. Mayrand-Provencher, D. Rochefort, Influence of the conductivity and viscosity of protic ionic liquids electrolytes on the e of RuO2 electrodes, J. Phys. Chem. C 113 (4) (2009) 1632–1639, https://doi.org/10.1021/jp8084149.
[8] L. Mayrand-Provencher, S. Lin, D. Lazzerini, D. Rochefort, Pyridinium-based protic ionic liquids as electrolytes for RuO2 electrochemical capacitors, J. Power Sources 195 (15) (2010) 5114–5121, https://doi.org/10.1016/j.jpowsour.2010.02.073.
[9] A. Scalia, et al., Electrolytes based on N-butyl-N-methyl-pyrrolidinium 4,5-dicyano-2-(Trifluoromethyl) imidazole for high voltage electrochemical double layer capacitors, ChemElectroChem 6 (2) (2019) 552–557, https://doi.org/10.1002/celc.201801172.
[10] A. Scalia, et al., High energy and high voltage integrated photo-electrochemical double layer capacitor, Sustain. Energy Fuels 2 (5) (2018) 968–977, https://doi.org/10.1039/c8se00003d.
[11] P. Zaccagnini, D. di Giovanni, M.G. Gomez, S. Passerini, A. Varzi, A. Lamberti, Flexible and high temperature supercapacitor based on laser-induced graphene electrodes and ionic liquid electrolyte, a de-rated voltage analysis, Electrochim. Acta 357 (2020), 136838, https://doi.org/10.1016/j.electacta.2020.136838.
[12] U.A. Rana, M. Forsyth, D.R. Macfarlane, J.M. Pringle, Toward protic ionic liquid and organic ionic plastic crystal electrolytes for fuel cells, Electrochim. Acta 84 (2012) 213–222, https://doi.org/10.1016/j.electacta.2012.03.058.
[13] H. Nakamoto, M. Watanabe, Brønsted acid-base ionic liquids for fuel cell electrolytes, Chem. Commun. (24) (2007) 2539–2541, https://doi.org/10.1039/b618953a.

[14] J. Snyder, K. Livi, J. Erlebacher, Oxygen reduction reaction performance of [MTBD] [beti]-encapsulated nanoporous NiPt alloy nanoparticles, Adv. Funct. Mater. 23 (44) (2013) 5494–5501, https://doi.org/10.1002/adfm.201301144.
[15] C. Wang, H. Luo, D.E. Jiang, H. Li, S. Dai, Carbon dioxide capture by superbase-derived protic ionic liquids, Angew. Chem. - Int. Ed. 49 (34) (2010) 5978–5981, https://doi.org/10.1002/anie.201002641.
[16] W. Xiong, M. Shi, L. Peng, X. Zhang, X. Hu, Y. Wu, Low viscosity superbase protic ionic liquids for the highly efficient simultaneous removal of H2S and CO2 from CH4, Sep. Purif. Technol. 263 (October) (2020) 2021, https://doi.org/10.1016/j.seppur.2021.118417.
[17] X. Zhu, M. Song, Y. Xu, DBU-based protic ionic liquids for CO2 capture, ACS Sustain. Chem. Eng. 5 (9) (2017) 8192–8198, https://doi.org/10.1021/acssuschemeng.7b01839.
[18] C.A. Summers, R.A. Flowers, Protein renaturation by the liquid organic salt ethylammonium nitrate, Prot. Sci. 9 (10) (2000) 2001–2008, https://doi.org/10.1110/ps.9.10.2001.
[19] D. Wakeham, et al., Surface structure of a 'non-amphiphilic' protic ionic liquid, Phys. Chem. Chem. Phys. 14 (15) (2012) 5106–5114, https://doi.org/10.1039/c2cp23694j.
[20] C. Largeot, C. Portet, J. Chmiola, P.L. Taberna, Y. Gogotsi, P. Simon, Relation between the ion size and pore size for an electric double-layer capacitor, J. Am. Chem. Soc. 130 (9) (2008) 2730–2731, https://doi.org/10.1021/ja7106178.
[21] P. Tamailarasan, S. Ramaprabhu, Carbon nanotubes-graphene-solidlike ionic liquid layer-based hybrid electrode material for high performance supercapacitor, J. Phys. Chem. C 116 (27) (2012) 14179–14187, https://doi.org/10.1021/jp302785j.
[22] C. Liu, Z. Yu, D. Neff, A. Zhamu, B.Z. Jang, Graphene-based supercapacitor with an ultrahigh energy density, Nano Lett. 10 (12) (2010) 4863–4868, https://doi.org/10.1021/nl102661q.
[23] L. Zhang, X.S. Zhao, Carbon-based materials as supercapacitor electrodes, Chem. Soc. Rev. 38 (9) (2009) 2520–2531, https://doi.org/10.1039/b813846j.
[24] A.A. Kornyshev, Double-layer in ionic liquids: paradigm change? J. Phys. Chem. B 111 (20) (2007) 5545–5557, https://doi.org/10.1021/jp067857o.
[25] M.Z. Bazant, B.D. Storey, A.A. Kornyshev, Double layer in ionic liquids: overscreening versus crowding, Phys. Rev. Lett. 106 (4) (2011) 6–9, https://doi.org/10.1103/PhysRevLett.106.046102.
[26] S.A. Kislenko, I.S. Samoylov, R.H. Amirov, Molecular dynamics simulation of the electrochemical interface between a graphite surface and the ionic liquid [BMIM] [PF_6], Phys. Chem. Chem. Phys. 11 (27) (2009) 5584–5590, https://doi.org/10.1039/b823189c.
[27] E. Paek, A.J. Pak, G.S. Hwang, A computational study of the interfacial structure and capacitance of graphene in [BMIM] [PF_6] ionic liquid, J. Electrochem. Soc. 160 (1) (2013) A1–A10, https://doi.org/10.1149/2.019301jes.
[28] C. Merlet, et al., On the molecular origin of supercapacitance in nanoporous carbon electrodes, Nat. Mater. 11 (4) (2012) 306–310, https://doi.org/10.1038/nmat3260.
[29] A. Fang, A. Smolyanitsky, Simulation study of the capacitance and charging mechanisms of ionic liquid mixtures near carbon electrodes, J. Phys. Chem. C 123 (3) (2019) 1610–1618, https://doi.org/10.1021/acs.jpcc.8b10334.
[30] X. Si, S. Li, Y. Wang, S. Ye, T. Yan, Effects of specific adsorption on the differential capacitance of imidazolium-based ionic liquid electrolytes, ChemPhysChem 13 (7) (2012) 1671–1676, https://doi.org/10.1002/cphc.201200013.
[31] A.P. Thompson, et al., LAMMPS - a flexible simulation tool for particle-based materials modeling at the atomic, meso, and continuum scales, Comput. Phys. Commun. 271 (2022), 108171, https://doi.org/10.1016/j.cpc.2021.108171.
[32] J. Wang, R.M. Wolf, J.W. Caldwell, P.A. Kollman, D.A. Case, Development and testing of a general Amber force field, J. Comput. Chem. 25 (9) (2004) 1157–1174, https://doi.org/10.1002/jcc.20035.
[33] K.G. Sprenger, V.W. Jaeger, J. Pfaendtner, The general AMBER force field (GAFF) can accurately predict thermodynamic and transport properties of many ionic liquids, J. Phys. Chem. B 119 (18) (2015) 5882–5895, https://doi.org/10.1021/acs.jpcb.5b00689.
[34] G.M.J. Barca, et al., Recent developments in the general atomic and molecular electronic structure system, J. Chem. Phys. 152 (15) (2020), https://doi.org/10.1063/5.0005188.
[35] C.I. Bayly, P. Cieplak, W.D. Cornell, P.A. Kollman, A well-behaved electrostatic potential based method using charge restraints for deriving atomic charges: the RESP model, J. Phys. Chem. 97 (40) (1993) 10269–10280, https://doi.org/10.1021/j100142a004.
[36] H. Liu, E. Maginn, A molecular dynamics investigation of the structural and dynamic properties of the ionic liquid 1-n-butyl-3-methylimidazolium bis (trifluoromethanesulfonyl) imide, J. Chem. Phys. 135 (12) (2011), https://doi.org/10.1063/1.3643124.
[37] F. Risplendi, F. Raffone, L.-C. Lin, J.C. Grossman, G. Cicero, Fundamental insights on hydration environment of boric acid and its role in separation from saline water, J. Phys. Chem. C 124 (2) (2020), https://doi.org/10.1021/acs.jpcc.9b10065.
[38] G. Tronci, F. Raffone, G. Cicero, Theoretical study of nanoporous graphene membranes for natural gas purification, Appl. Sci. 8 (9) (2018), https://doi.org/10.3390/app8091547.
[39] L.C. Lin, J.C. Grossman, Atomistic understandings of reduced graphene oxide as an ultrathin-film nanoporous membrane for separations, Nat. Commun. 6 (2015) 1–7, https://doi.org/10.1038/ncomms9335.
[40] F. Raffone, F. Savazzi, G. Cicero, Molecular dynamics study of the pore formation in single layer graphene oxide by a thermal reduction process, Phys. Chem. Chem. Phys. 23 (20) (2021) 11831–11836, https://doi.org/10.1039/d1cp00134e.
[41] F. Raffone, F. Savazzi, G. Cicero, Controlled pore generation in single-layer graphene oxide for membrane desalination, J. Phys. Chem. Lett. 10 (23) (2019), https://doi.org/10.1021/acs.jpclett.9b03255.
[42] F. Raffone, G. Cicero, Unveiling the fundamental role of temperature in RRAM switching mechanism by multiscale simulations, ACS Appl. Mater. Interfaces 10 (8) (2018), https://doi.org/10.1021/acsami.8b00443.
[43] C. Noh, Y. Jung, Understanding the charging dynamics of an ionic liquid electric double layer capacitor: via molecular dynamics simulations, Phys. Chem. Chem. Phys. 21 (13) (2019) 6790–6800, https://doi.org/10.1039/c8cp07200k.
[44] Y.J. Tu, S. Delmerico, J.G. McDaniel, Inner layer capacitance of organic electrolytes from constant voltage molecular dynamics, J. Phys. Chem. C 124 (5) (2020) 2907–2922, https://doi.org/10.1021/acs.jpcc.0c00299.
[45] V. Lockett, R. Sedev, S. Harmer, J. Ralston, M. Horne, T. Rodopoulos, Orientation and mutual location of ions at the surface of ionic liquids, Phys. Chem. Chem. Phys. 12 (41) (2010) 13816–13827, https://doi.org/10.1039/c0cp00683a.
[46] V. Lockett, R. Sedev, C. Bassell, J. Ralston, Angle-resolved X-ray photoelectron spectroscopy of the surface of imidazolium ionic liquids, Phys. Chem. Chem. Phys. 10 (9) (2008) 1330–1335, https://doi.org/10.1039/b713584j.
[47] A.P. Willard, D. Chandler, The molecular structure of the interface between water and a hydrophobic substrate is liquid-vapor like, J. Chem. Phys. 141 (18) (2014), https://doi.org/10.1063/1.4897249.
[48] A.V. Rudnev, K. Kiran, P. Broekmann, Specific cation adsorption: exploring synergistic effects on CO2 electroreduction in ionic liquids, ChemElectroChem 7 (8) (2020) 1897–1903, https://doi.org/10.1002/CELC.202000223.